Analytical Methods

Accepted Manuscript

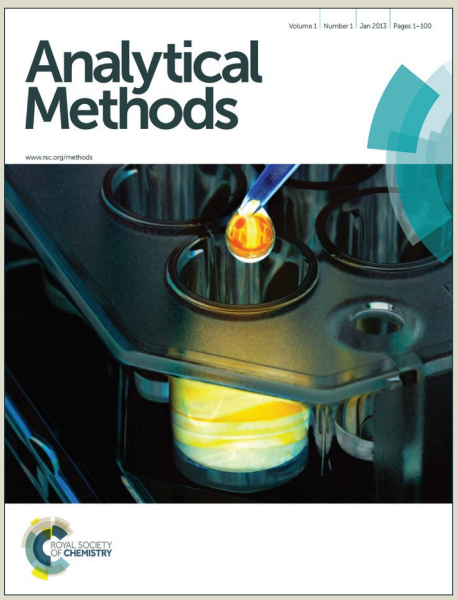

This is an *Accepted Manuscript*, which has been through the Royal Society of Chemistry peer review process and has been accepted for publication.

Accepted Manuscripts are published online shortly after acceptance, before technical editing, formatting and proof reading. Using this free service, authors can make their results available to the community, in citable form, before we publish the edited article. We will replace this *Accepted Manuscript* with the edited and formatted *Advance Article* as soon as it is available.

You can find more information about *Accepted Manuscripts* in the Information for Authors.

Please note that technical editing may introduce minor changes to the text and/or graphics, which may alter content. The journal's standard Terms & Conditions and the Ethical guidelines still apply. In no event shall the Royal Society of Chemistry be held responsible for any errors or omissions in this *Accepted Manuscript* or any consequences arising from the use of any information it contains.

ROYAL SOCIETY OF CHEMISTRY

www.rsc.org/methods

Keywords

ultrafiltration; mass spectrometry; PTP1B inhibitor; traditional medicine, Chinese red yeast rice; monascorubramine.

Introduction

Traditional medicines, which are derived from various sources, are recognized as complex chemical libraries possessing multiple pharmacological activities. However, the beneficial and/or hazardous effects of such medicines are caused by specific bioactive compounds that constitute only a minute portion of the crude drugs[1]. The mainstream method for screening bioactive compounds from traditional medicines is bioassay-guided isolation. This technique is straightforward and well established, although it is laborious and time-consuming[2, 3]. This method also causes significant loss of bioactive compounds during the separation, refining and drying processes. Moreover, the usage of crude drugs instead of single extracted active compounds has received significant attention because such drugs possess multiple active components that may operate synergistically within a traditional medicine, producing desirable pharmacological activities and lowering the chances of adverse effects[4].

Abbreviation: LC-MS, liquid chromatography-mass spectrometry; PTP1B, protein tyrosine phosphatase 1B; MS^{E}, mass spectrometry$^{Elevated\ Energy}$; TCPTP, T cell protein tyrosine phosphatase; PCSK9, proprotein convertase subtilisin /kexin type 9; LDLR, low-density lipoprotein receptor; PMM2, phosphomannomutase 2; SHMT, serine hydroxymethyltransferase; BRD4-1, bromodomain-containing protein 4 domain 1; JMJD2A, jumonji domain containing 2A.

Many effective analysis tools have been used to screen potential bioactive compounds from crude drugs without isolation, including the coupling of chromatographic and spectroscopic techniques[2, 5, 6]. Liquid chromatography-mass spectrometry (LC-MS) is commonly employed for such purposes due to its powerful liquid-phase separation efficiency combined with its sensitive and accurate mass detection[7-9]. Ultrafiltration-based LC-MS screening, which can be paired with various affinity selection strategies to directly assess the binding characteristics of candidates to macromolecular targets[2, 3, 10-12], is particularly useful in this regards, as it is fast, inexpensive, and reliable. Additionally, this technique can be applied to any type of soluble macromolecular target type regardless of its function[13, 14]. During the ultrafiltration-based LC-MS screening, ultrafiltration is used as a sieving mechanism for separating protein-ligand complexes from unbound small molecules after ligands in the mixture are bound to the target protein. Following this, the protein-ligand complexes are dissociated, and LC-MS and/or LC-MS/MS are employed to analyze and identify active compounds within them. Because of its speed and accuracy, ultrafiltration-based LC-MS technique is most frequently utilized in primary screening of compounds libraries; however, this technique often produces false-positive results. Conventionally, the potential active

compounds are selected from compounds libraries, and then confirmed by competition binding with positive controls, demonstrating the binding selectivity of compounds with regard to other targets. Alternatively, isolated compounds can also be evaluated using bioassay. However, a major challenge in using ultrafiltration-based LC-MS technique to screen traditional medicine is that false-positive results cannot be easily separated from an overall crude drug profile[13].

To address this limitation, we modified the analytical method of using the ultrafiltration-based LC-MS approach to screen bioactive compounds and distinguish false-positive results in compounds mixtures, particularly in traditional medicines. To accomplish this, we first used *in vitro* enzymatic assays to screen various crude extracts of traditional medicines for their abilities to inhibit protein tyrosine phosphatase 1B (PTP1B). PTP1B is a prototype non-receptor cytoplasmic PTPase enzyme that negatively regulates insulin and leptin signaling pathways[15, 16]. Then, we utilized an off-line ultrafiltration-based affinity selection combined with the LC-MS screening approach developed by Comess[13] (**Fig. 1**) to screen the potential bioactive compounds in Chinese red yeast rice (RYR). We found this method is straightforward and does not require compound isolation. Based on our

findings, RYR exhibited PTP1B inhibitory properties. According to our analysis, at least one compound in the RYR crude extract was identified as a potential PTP1B inhibitor, and its structure was further confirmed using mass spectrometry$^{\text{Elevated Energy}}$ (MS^{E}). Additionally to verify the selectivity of this potential PTP1B inhibitor, we determined its binding abilities to a homologous protein of PTP1B and several randomly selected proteins.

(Please insert Fig. 1)

Materials and Methods

Materials and chemicals

Chinese RYR powder was purchased from Hongjiuqu Ltd. (Fujian, China). Positive and negative controls named FL+ve and FL-ve, respectively (**Fig. 2**j, k) were provided by Fu laboratory in the School of Pharmacy at Shanghai Jiao Tong University (Shanghai, China).

PTP1B (40 kDa), T cell protein tyrosine phosphatase (TCPTP, 45 kDa), proprotein convertase subtilisin/kexin type 9 (PCSK9, 70 kDa), low-density lipoprotein receptor (LDLR, 11 kDa), phosphomannomutase 2 (PMM2, 28 kDa), serine hydroxymethyltransferase (SHMT, 50 kDa), bromodomain-containing protein 4 domain 1 (BRD4-1, 15 kDa), and jumonji

domain-containing 2A (JMJD2A, 50 kDa) were purified and provided by Viva Biotech Ltd. (Shanghai, China). Standard sodium orthovanadate (SOV) was purchased from Sigma-Aldrich (Missouri, US). Water was purified in-house using a Milli-Q water purification system (Milford, MA). Para-nitrophenylphosphate (*p*-NPP), dissolving buffer, and all other chemicals and solvents otherwise not mentioned were provided by Viva Biotech Ltd. (Shanghai, China).

Sample preparation

In total, 10 g of RYR rice was treated with 70% ethanol (EtOH) (3 times for 2 hr each) at 40 ℃ to obtain the crude RYR extract. The three crude extracts were combined and evaporated under a vacuum at 40 ℃. The RYR crude extract was concentrated by dissolving it in dimethyl sulfoxide (DMSO) to achieve a final concentration of 40 mg/mL. The solution was then filtered through a 0.22-μm filter and stored at 4 ℃.

Enzyme activity assay

For the inhibition assay, aliquots of the RYR crude extract solution (40 mg/mL in DMSO)

were mixed with purified enzymes (either 7.5 μg/mL recombinant PTP1B or 2.5 μg/mL recombinant TCPTP) in the assay buffer (10 mM Tris at pH 7.5, 25 mM NaCl, 1 mM EDTA) and was then incubated for 10 min at 37 °C. Following this, 6 mM *p*-NPP was then added to the mixtures, and incubation continued at 37 °C for 20 min. Subsequently, each reaction was quenched with distilled H_2O, and absorbance was measured at 405 nm using a Varioskan® Flash Multimode Reader (Thermo Scientific, USA). IC_{50} measurements were derived from three independent experiments measuring the inhibitory activities of the extract using the following linear concentration gradients: of 1 mg/mL, 0.8 mg/mL, 0.6 mg/mL, 0.4 mg/mL, 0.2 mg/mL, and 0.1 mg/mL. IC_{50} was calculated using SPSS version 22.0 (SPSS Inc., Chicago, IL, USA, www.spss.com). SOV and FL+ve[17] (**Fig. 2**j) were used as the positive controls. The inhibitory effect was calculated as follows:

$$\text{Inhibition (\%)} = (A_1 - A_2)/A_1 \times 100\% \quad (1)$$

where A_1 is the absorbance of the control, and A_2 is the absorbance of the sample.

LC-MS and LC-MS^E analytical conditions

Ultra-performance liquid chromatography (UPLC) was performed using a Waters ACQUITY

UPLC system (waters, Milford, MA, USA) with an ACQUITY UPLC BEH C18 column (2.1× 50 mm, 1.7 μm). The solvents used were as follows: A, 0.1% diluted aqueous formic acid; and B, 100% acetonitrile (ACN). The gradient conditions for LC-MS were as follows: 0–1 min, 2→5% B; 1–9 min, 5→90% B; and 9–10 min, 95% B. The gradient conditions for LC-MS^E were as follows: 0–2 min, 2→5% B; 2–27 min, 30→70% B; 27–29 min, 70→90% B; and 29–30 min, 90% B. The injection volume was 5 μL, and the column and sample temperatures were maintained at 40 ℃ and 5 ℃, respectively.

Mass spectrometric detection was coupled with UPLC and performed using a Synapt™ quadrupole time-of-flight (Q-TOF) High-Definition Mass Spectrometer (Waters, Milford, MA, USA) equipped with an electrospray ionization (ESI) source operating in positive ionization mode. The optimized mass spectrometric parameters were determined as follows: capillary voltage, 2.5 kV; sample cone, 25 V; extraction cone, 4.0 V; source temperature, 120 ℃; and desolvation temperature, 400 ℃. Nitrogen was used as a desolvation and a cone gas at a flow rate of 600 and 50 L/h, respectively. Argon was used as a collision gas. A lock mass of leucine-enkephalin at a concentration of 200 pg/mL in 50% ACN-water solution (including 0.1% formic acid) was employed as an external reference to generate a $[M+H]^+$

ion in positive mode at *m/z* 556.2771 via a lock spray interface at a flow rate of 5 µL/min to acquire accurate mass during the analysis. The sample was scanned in full-scan mode from *m/z* 80 to 800 in 1 sec scan intervals.

The LC-MS^E analysis was performed with two scan functions: 6 eV for the low collision energy scan and a collision energy ramp of 40–80 eV for the high-collision energy scan. The molecular ion data were scanned from *m/z* 50 to 800 in 1 sec scan intervals. Masslynx software (Waters, Milford, MA) was used to integrate and visually inspect the peaks.

Ultrafiltration-based affinity selection

The methodology has been described by Comess[13] (**Fig. 1**). PTP1B was analyzed at 10, 20 and 30 µM in parallel. TCPTP, PCSK9, LDLR, PMM2, SHMT, BRD4-1, and JMJD2A were analyzed at 30 µM. Prior to screening, 100 µg/mL of the RYR crude extract and 5 µM of each FL+ve and FL-ve (**Fig. 2**j, k) were well mixed with PTP1B in Tris buffer for 30 min at room temperature. 100 µg/mL RYR extract and 5 µM negative control (**Fig. 2**k) were mixed with TCPTP, PCSK9, LDLR, PMM2, SHMT, BRD4-1, or JMJD2A, respectively, for 30 min at room temperature to assess the selectivity of the PTP1B bound ligands.

In total, 450 μL of each protein-ligand mixture was transferred to the centrifugal concentrators containing a Vivacon® 500 filter unit (30,000 molecular weight cutoff (MWCO); 10,000 MWCO) (Sartorius Stedim Biotech, Germany). A 50 μL fraction of the protein-ligand mixture (R0) was collected prior to centrifugal filtration was reserved for mass spectrometric detection. After centrifugation for 10 min at 12,000 rpm using a MicroCL 17 microcentrifuge (Thermo Scientific™, Rockford, IL, USA) at room temperature, 400 μL of the solution was filtered through the MWCO membrane, and 50 μL was left on top of the filter membrane. The retentate was restored to 500 μL by adding 450 μL of Tris buffer. The samples were re-mixed and then re-filtered two more times via ultrafiltration to collect the final 50 μL of retentate (R3) on top of the filter membrane. The compounds in R0 and R3 were released by adding 150 μL of 100% ACN for protein denaturation. The sample was then centrifuged at 12,000 rpm for 4 min. In total, 160 μL of each supernatant with the released compounds was collected and transferred to a 96-deep-well plate for mass spectrometric detection. A control experiment with no protein was also performed for each screening experiment by collecting samples as $R0^-$ and $R3^-$.

The compounds released in $R3^+$ after mass spectrometric detection were dried, re-dissolved

in ACN/water (50:50; vol:vol) and were identified using LC- MS^E.

Evaluation criteria for the binding behavior

A set of four LC-MS profiles was created: the unprocessed RYR crude extract prior to centrifugal filtration ($R0^-$), the RYR crude extract mixed with PTP1B prior to affinity selection ($R0^+$), the released compounds from the unprocessed RYR crude extract after ultrafiltration ($R3^-$), and the free compounds produced after the affinity selection ($R3^+$). These profiles were collected and analyzed for each possible candidate compound contained within RYR. Specific binding was then determined based on the difference between the $R3^+/R0^+$ and $R3^-/R0^-$ ratio (Equation 2), where R3/R0 corresponded to a comparison between the peak heights in the LC-MS chromatogram of each candidate before and after the ultrafiltration-based affinity selection. Theoretically, the value of the parallel negative control (*i.e.*, $(R3^- / R0^-) \times 100\%$) for each candidate should be approximately equal to 0.1% because 90% of the volume is filtered out over each cycle. In this case, the RB value of a 100% bound ligand would be approximately equal to 1000% because the ligand is 10-fold concentrated in the $R3^+$ profile versus the $R0^+$ profile. In other words, a candidate would have a calculated

RB value between 0% and 1000% depending on its binding strength. Experimentally, a candidate with an RB value higher than 20% would be considered a possible bound ligand requiring further confirmation.

$$\text{Relative Binding \% (RB\%)} = [(R3^{+}/R0^{+}) \times 100\%] - [(R3^{-}/R0^{-}) \times 100\%] \quad (2)$$

False-positive compounds, which may aggregate, or non-specifically bind to either enzyme or artifacts, can be determined according to the retention factor (R*f*) calculated as shown in Equation 3. Theoretically, a false-positive compound would have an R*f* value approximately equal to 1 because similar amounts of the compound would be retained in both the $R3^{+}$ and $R3^{-}$ profiles. In this case, a compound designated as a possible ligand according to Equation 2 with a significantly higher R*f* value (*i.e.,* R*f* > 10) according to Equation 3 would be a reliable active ligand.

$$\text{Retention Factor (R}f\text{)} = [(R3^{+}/R0^{+}) \times 100\%]/[(R3^{-}/R0^{-}) \times 100\%] \quad (3)$$

Results and Discussion

RYR crude extract exhibits potent PTP1B inhibition activity

RYR is a traditional medicine that has been used as a functional food due to its

cholesterol-lowering property. Many bioactive constituents of RYR have been discovered[18-20]. Recent studies have shown that RYR can reduce plasma glucose levels in streptozotocin (STZ)-induced diabetic animals by enhancing insulin secretion[21, 22]; however, the mechanism underlying the hypoglycemic effect produced by RYR remains unknown. Our enzyme inhibition assay results showed that the RYR crude extract displayed an average IC_{50} value of 7.56 μg/mL against PTP1B **(Table 1**), suggesting that RYR may enhance insulin secretion via inhibiting PTP1B.

(Please insert Table 1)

The majority of known PTP1B inhibitors frequently cause lethal adverse effects because they also affect the normal function of TCPTP, which shares 72% of its catalytic domain sequence with PTP1B[23]. In addition, a lack of TCPTP activity may lead to hematopoietic defects and anemia[24, 25]. By comparing the inhibitory effects of the RYR crude extract on PTP1B and TCPTP (IC_{50} = 49.9 μg/mL) (**Table 1**), our results demonstrate that RYR exhibited moderate selectivity toward PTP1B over TCPTP.

Ultrafiltration-based LC-MS screening

A general method of the ultrafiltration-based LC-MS approach has three steps: protein-ligand equilibrium, affinity selection, and compound identification[13, 14] (**Fig. 1**). In the current study, RYR crude extract, which contains a mixture of candidates, was injected into an ultrafiltration chamber to allow the extract to reach a solution-binding equilibrium with PTP1B. To date, 35 small molecule compounds have been identified in RYR[26-28]. In our preliminary experiments, the lowest detectable concentration of the RYR crude extract for the ultrafiltration-based LC-MS method was 100 μg/mL. This limit of detection allowed us to identify 8 of the 35 known compounds by comparing our mass spectra with the literature spectra (**Fig. 2**a-h, **Table 2**)[26-28]. The remainder of the known compounds may have been poorly extracted, had poor sensitivity to the electrospray ionization, or underwent degradation during the extraction process and/or storage. Despite that some distinct $[M+H]^+$ ions that potentially corresponded to unknown compounds were also found when analyzing and comparing our mass spectra with the literature spectra, we only focused on the identified compounds in this current study. This was because the aim of our work was to validate the utility of our modified ultrafiltration-based affinity screening method and to verify that our evaluation criteria for the binding behavior were workable for screening potential compounds

from traditional medicine without separation.

In methods such as ours, ligands and protein concentrations also determine the number of ligands that can be obtained[13, 14]. Typically, the concentration of a target macromolecule is kept in excess of each individual ligand candidate. This enables a high number of potential ligands to be detected while minimizing the competition between ligands with different binding strengths and for the development of a ranking scale for the active ligands with different binding strengths. In this case, we screened the RYR crude extract with FL+ve and FL-ve (**Fig. 2**j,k) in the presence of 10, 20 and 30 μM PTP1B to ensure that active ligands with both high and lower affinity could be observed[29]. During affinity selection, the ultrafiltration chamber separated out the protein-ligand complexes from the protein and compound mixture by eluting unbound ligands away from the chamber. Three rounds of affinity filtration were able to increase the signal-to-noise ratio of the bound ligands over the background, enabling them to be easily detectable[13]. In theory, after multiple rounds of filtration and re-equilibration, the ultrafiltration membrane should retain only PTP1B and PTP1B-ligand complexes. The ligands were then identified based on their corresponding mass spectrometric peak positions, and the binding strength of each ligand was determined

using Equation 2.

(Please insert Fig. 2 and Table 2)

As shown in **Table 2**, the presence of FL+ve (**Fig. 2**j)[17] and FL-ve (**Fig. 2**k) in the mixture with RYR and 10 μM PTP1B indicated that this screening functioned appropriately. Compared with FL+ve, two compounds in the RYR extract, monascorubramine (**Fig. 2**d) and monasfluor B (**Fig. 2g**), exhibited relatively weak affinity for 10 μM PTP1B ($RB_{(monascorubramine)}$ = 52.49%; $RB_{(monasfluor\ B)}$ = 48.36%). However, monasfluor B may not be a reliable active ligand for PTP1B due to its low retention factor ($Rf_{(monasfluor\ B)}$ = 1.46). Due to the specific chemical properties of compounds in mixtures, promiscuous compounds are retained on top of the ultrafiltration membranes, which lead to false-positive results. Therefore, R*f* value is calculated to determine the reliability of an RB value (Equation 3). This simple calculation provides an effective approach for identifying reliable active ligands from the results.

When the concentration of PTP1B was increased from 20 to 30 μM, the RB value of FL+ve did not improve, whereas the RB value of monascorubramine steadily increased to 87.82% and further to 119.22% (**Table 2**). This result clearly indicated that FL+ve was a

comparatively stronger PTP1B inhibitor than the potential ligands in the RYR crude extract; therefore, FL+ve significantly competed against the weaker ligands, reducing their detectability at a low concentration of PTP1B (*i.e.*, 10 μM). By increasing the protein concentration, the weaker ligands were more easily identifiable in addition to the high-affinity compounds. Thus, monascorubramine was identified as a bioactive compound with a moderate binding affinity for PTP1B. Additionally, we demonstrated that monasfluor B is a promiscuous compound because its R*f* values in the presence of 20 and 30 μM PTP1B did not improve compared to that obtained in the presence of 10 μM PTP1B; although its slightly increased RB values suggest that monasfluor B may be a weak PTP1B ligand (**Table 2**). Another ligand, monascopyridine B (**Fig. 2**e), was observed when the concentration of PTP1B was increased to 30 μM, but it was also determined to be a promiscuous compound because of the aforementioned concerns.

Structural characterization of the PTP1B inhibitor from the RYR extract using MS^E

In total, 8 of 35 identified compounds (**Fig. 2**a–h) in the RYR crude extract were found by comparing our acquired mass spectra with the published literature[26-28]. Additionally, we

identified monascorubramine as an active component in the RYR crude extract that can bind to PTP1B. Conventional methods would have used chromatographic separation techniques to isolate and identify bioactive compounds after they have been successfully tracked[8]. In the current study, we presented an accurate and effective tool, MS^E, that supported the use of ultrafiltration-based LC-MS screening approach in characterizing the structures of active compounds screened from RYR crude extract without separation in a single affinity selection run.

MS^E is an intelligent approach for obtaining both the pseudo-molecular and the fragmental ion information for compounds in a single analytical run[30]. MS^E of the $[M+H]^+$ ion (*m/z* 382.2012) of monascorubramine was found at *m/z* = 338.2120, which matched the loss of a carbon dioxide from the $[M+H]^+$ (**Table 3**, **Fig. 4**a, c); another fragment ion, $[M - C_8H_{14}O + H]^+$ at *m/z* = 256.0973, was generated by loss of a long keto-aliphatic chain, $C_8H_{14}O$, from the precursor ion (**Table 3**, **Fig. 4**b, c). Further loss of a carbon dioxide yielded the fragment ion $[M - C_8H_{14}O\text{-}CO_2 + H]^+$ at *m/z* = 212.1063. Hence, the relevant precursor and fragments were linked together by a mass defect. This confirms that the potential ligand for PTP1B was monascorubramine.

(Please insert Table 3 and Fig. 4)

Selectivity of the PTP1B inhibitor

Monascorubramine is one of the major secondary metabolites produced by *Monascus purpureus*, which was first isolated by Martínková[31]. To the best of our knowledge, our report is the first to identify monascorubramine as one of the potentially active compounds in RYR for PTP1B inhibition. To determine whether monascorubramine possessed selective binding affinity towards PTP1B, we analyzed its binding behaviors to TCPTP and 6 other randomly chosen proteins using the ultrafiltration-based LC-MS screening approach. **Table 4** shows the binding behaviors of monascorubramine to 7 proteins, including TCPTP, PCSK9, LDLR, PMM2, SHMT, BRD4-1, and JMJD2. These results clearly indicate that monascorubramine is a specific ligand for PTP1B because it exhibited negligible binding affinity to the random proteins. Additionally, monascorubramine demonstrated a 5-fold decrease in affinity for 30 μM TCPTP (RB = 21.54%) compared with its binding affinity for 30 μM PTP1B (RB = 119.22%). This result was positively related to the outcome of the enzyme inhibition assay used to evaluate RYR crude extract to TCPTP (IC_{50} = 44.1 μg/mL) and PTP1B (IC_{50} = 7.56

μg/mL). Thus, monascorubramine was identified as a potential selective PTP1B inhibitor in RYR, and could be, partially, responsible for the anti-diabetic activity of RYR.

(Please insert Table 4)

Conclusion

In the present study, we used a traditional medicine, Chinese RYR, as a representative mixture of compounds and applied an efficient ultrafiltration-based LC-MS approach for rapid screening of the PTP1B inhibitors directly from this traditional medicine. To the best of our knowledge, this is the first report to demonstrate that the Chinese RYR possesses inhibitory activity toward PTP1B and that the anti-diabetic effect of Chinese RYR is partially dependent on the potential PTP1B inhibitory activity of monascorubramine. We also optimized criteria for assessing binding strength of each possible ligand and for estimating false-positive results. The proposed ultrafiltration-based LC-MS screening approach coupled with our optimized analytical method is thus predicted to facilitate the screening of active compounds from complex chemical libraries, especially traditional medicines without separation.

Acknowledgements

The authors gratefully acknowledge the financial support from the National Natural Science Foundation of China (81202397), the Shanghai Natural Science Foundation Project of China (12ZR1415400), and the International S&T Cooperation Program of China (2014DFA41360). The authors would also like to thank Dongming Qian, Yu Xia at Viva Biotech Ltd., and both the senior students and researchers from Fu laboratory in the School of Pharmacy of Shanghai Jiao Tong University for their valuable help.

Reference

1. P. Dražar and J. Moravcova, *Journal of Chromatography B*, 2004, **812**, 3-21.
2. G. Z. Xin, J. L. Zhou, L. W. Qi and P. Li, *Comb Chem High Throughput Screen*, 2011, **14**, 93-103.
3. O. Potterat and M. Hamburger, *Natural Product Reports*, 2013, **30**, 546-564.
4. S. W. Yoon, J. S. Jeong, J. H. Kim and B. B. Aggarwal, *Integr Cancer Ther*, 2013, **13**, 310-331.
5. Z. M. Qian, S. J. Qin, L. Yi, H. J. Li, P. Li and X. D. Wen, *Biomed Chromatogr*, 2008, **22**, 202-206.
6. J. L. Zhou, Z. M. Qian, Y. D. Luo, D. Tang, H. Chen, L. Yi and P. Li, *Biomed Chromatogr*, 2008, **22**, 1164-1172.
7. C. F. de Jong, R. J. Derks, B. Bruyneel, W. Niessen and H. Irth, *J Chromatogr A*, 2006, **1112**, 303-310.

8. R. B. van Breemen, Y. Tao and W. Li, *Fitoterapia*, 2011, **82**, 38-43.
9. Y. Choi, K. Jermihov, S. J. Nam, M. Sturdy, K. Maloney, X. Qiu, L. R. Chadwick, M. Main, S. N. Chen, A. D. Mesecar, N. R. Farnsworth, G. F. Pauli, W. Fenical, J. M. Pezzuto and R. B. van Breemen, *Anal Chem*, 2011, **83**, 1048-1052.
10. R. B. van Breemen, C. R. Huang, D. Nikolic, C. P. Woodbury, Y. Z. Zhao and D. L. Venton, *Anal Chem*, 1997, **69**, 2159-2164.
11. H. P. Song, J. Chen, J. Y. Hong, H. Hao, L. W. Qi, J. Lu, Y. Fu, B. Wu, H. Yang and P. Li, *Chem Commun (Camb)*, 2015, **51**, 1494-1497.
12. Z. Yang, Y. Zhang, L. Sun, Y. Wang, X. Gao and Y. Cheng, *Anal Chim Acta*, 2012, **719**, 87-95.
13. K. M. Comess, M. E. Schurdak, M. J. Voorbach, M. Coen, J. D. Trumbull, H. Yang, L. Gao, H. Tang, X. Cheng, C. G. Lerner, J. O. McCall, D. J. Burns and B. A. Beutel, *J Biomol Screen*, 2006, **11**, 743-754.
14. K. M. Comess, J. D. Trumbull, C. Park, Z. Chen, R. A. Judge, M. J. Voorbach, M. Coen, L. Gao, H. Tang, P. Kovar, X. Cheng, M. E. Schurdak, H. Zhang, T. Sowin and D. J. Burns, *J Biomol Screen*, 2006, **11**, 755-764.
15. M. F. White and C. R. Kahn, *J Biol Chem*, 1994, **269**, 1-4.
16. B. P. Kennedy, *Biomed Pharmacother*, 1999, **53**, 466-470.
17. J. Liu, F. Jiang, Y. Jin, Y. Zhang, J. Liu, W. Liu and L. Fu, *Eur J Med Chem*, 2012, **57**, 10-20.
18. D. Heber, I. Yip, J. M. Ashley, D. A. Elashoff, R. M. Elashoff and V. L. Go, *Am J Clin Nutr*, 1999, **69**, 231-236.
19. A. Endo, *J Antibiot (Tokyo)*, 1980, **33**, 334-336.
20. M. Journoud and P. J. Jones, *Life Sci*, 2004, **74**, 2675-2683.
21. C.-F. Su, I. M. Liu and J.-T. Cheng, *Food Chemistry*, 2007, **104**, 45-52.
22. C.-C. Chen and I. M. Liu, *Neuroscience Letters*, 2006, **404**, 117-121.
23. T. Tiganis, *Febs j*, 2013, **280**, 445-458.
24. K. E. You-Ten, E. S. Muise, A. Itie, E. Michaliszyn, J. Wagner, S. Jothy, W. S. Lapp and M. L. Tremblay, *J Exp Med*, 1997, **186**, 683-693.
25. K. M. Heinonen, F. P. Nestel, E. W. Newell, G. Charette, T. A. Seemayer, M. L. Tremblay and W. S. Lapp, *Blood*, 2004, **103**, 3457-3464.
26. Y. L. Lin, T. H. Wang, M. H. Lee and N. W. Su, *Appl Microbiol Biotechnol*, 2008, **77**,

965-973.

27. P. Patakova, *J Ind Microbiol Biotechnol*, 2013, **40**, 169-181.

28. J. Ma, Y. Li, Q. Ye, J. Li, Y. Hua, D. Ju, D. Zhang, R. Cooper and M. Chang, *J Agric Food Chem*, 2000, **48**, 5220-5225.

29. H. Li, F. Song, J. Xing, R. Tsao, Z. Liu and S. Liu, *J Am Soc Mass Spectrom*, 2009, **20**, 1496-1503.

30. R. S. Plumb, K. A. Johnson, P. Rainville, B. W. Smith, I. D. Wilson, J. M. Castro-Perez and J. K. Nicholson, *Rapid Commun Mass Spectrom*, 2006, **20**, 1989-1994.

31. L. Martínková, P. J˚zlová and D. Veselý, *Journal of Applied Bacteriology*, 1995, **79**, 609-616.

Tables

Table 1

In vitro inhibitory activity against two PTPs of RYR crude extract

Samples	IC50[a]	
	PTP1B	TCPTP
RYR crude extract	7.56 μg/mL	44.1 μg/mL
FL+ve[b]	2.4 μM	9.7 μM
SOV[b]	0.046 μM	0.014 μM

[a] IC_{50} values are means of three independent experiments

[b] SOV and FL+ve [17] are positive controls

Table 2

Binding abilities of compounds in 100 μg/mL RYR crude extract to PTP1B

No.	Name	MW	$[M+H]^+$ *m/z*	Rt(min)	PPM	10 μM PTP1B		20 μM PTP1B		30 μM PTP1B	
						RB (%)[a]	R*f*[a]	RB (%)[a]	R*f*[a]	RB (%)[a]	R*f*[a]
2a	monascin	358.178	359.1858	6.17	0.8	5.58	1.16	13.32	1.37	22.89	1.65
2b	ankaflavin	386.2093	387.2171	6.75	-3.4	<0	<1	<0	<1	<0	<1
2c	rubropunctamine	353.1627	354.1705	4.91	2	1.84	2.51	5.03	5.1	6.65	4.73
2d	monascorubramine	381.194	382.2018	5.63	-0.3	52.49	14.42	87.82	20.13	119.22	30.21
2e	monascopyridine B	383.2097	384.2097	6.42	2.3	6.39	1.06	31.05	1.28	38.48	1.35
2f	monasfluor A	356.1624	357.1702	5.89	-0.6	5.55	1.3	12.69	1.73	15.68	1.9
2g	monasfluor B	384.1937	385.2015	6.55	-0.5	48.36	1.46	45.05	1.41	63.22	1.62
2h	compound R3	374.1729	375.1808	4.78	-3.2	1.73	4.49	0.04	1.08	<0	<1
2j	FL+ve[b]	564.1753	565.1851	6.24	3.5	422.42	69.1	453.4	74	428.06	70.51
2k	FL-ve [c]	468.0132	469.0193	5.415	-3.8	<0	<1	<0	2.499	1.88	8.452

[a] RB and R*f* values are the average of three independent experiments

[b] FL+ve with IC_{50} = 2.4 μM[17]

[c] FL-ve with IC_{50}> mM

Table 3

Accurate product ions mass data of monascorubramine

$[M+H]^+$		PPM	Formula element	Fragment ions
Measured *m/z*	Calculated *m/z*			
382.2021	382.2018	0.8	$C_{23}H_{27}NO_4$	$[M+H]^+$
338.2111	338.212	-2.7	$C_{22}H_{27}NO_2$	$[M-CO_2+H]^+$
256.0973	256.0974	-0.4	$C_{15}H_{13}NO_3$	$[M-C_8H_{14}O+H]^+$
212.1063	212.1075	-5.7	$C_{14}H_{13}NO$	$[M-C_8H_{14}O-CO_2+H]^+$

Table 4

Binding behaviors of monascorubramine to TCPTP and 6 randomly chosen proteins

Protein[b] (30 μM)	Monascorubramine in 100 μg/mL RYR extract	
	RB (%)[a]	R*f*[a]
TCPTP	21.54	3.08
PCSK9	20.87	12.13
LDLR	<0	<1
PMM2	2.08	1.28
SHMT	16.97	3.24
BRD4-1	21.78	3.88
JMJD2A	<0	<1

[a] RB and R*f* values are the average of three independent experiments

[b]RB values of FL-ve to each protein < 0

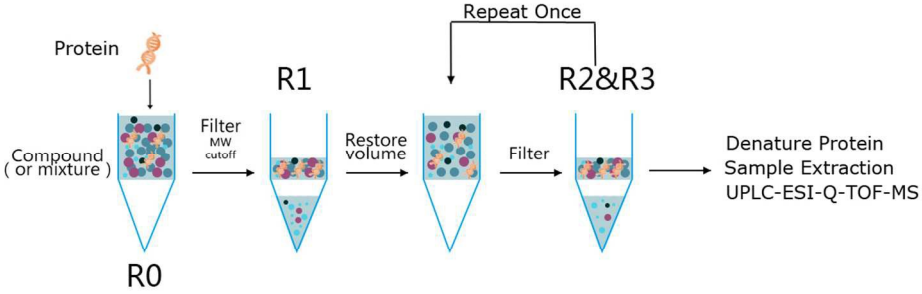

Fig. 1. Schematic of the ultrafiltration-based affinity selection. Compounds are initially mixed and incubated with the target protein in a tube at equilibrium. The volume of the mixture is repeatedly decreased to one-tenth of the initial volume followed by 3 rounds of ultrafiltration to enrich bound ligands over the non-bound compounds and to reduce the chemical background. The samples are taken before (R0) and after (R3) 3 rounds of ultrafiltration for mass spectrometric analysis.
457x174mm (72 x 72 DPI)

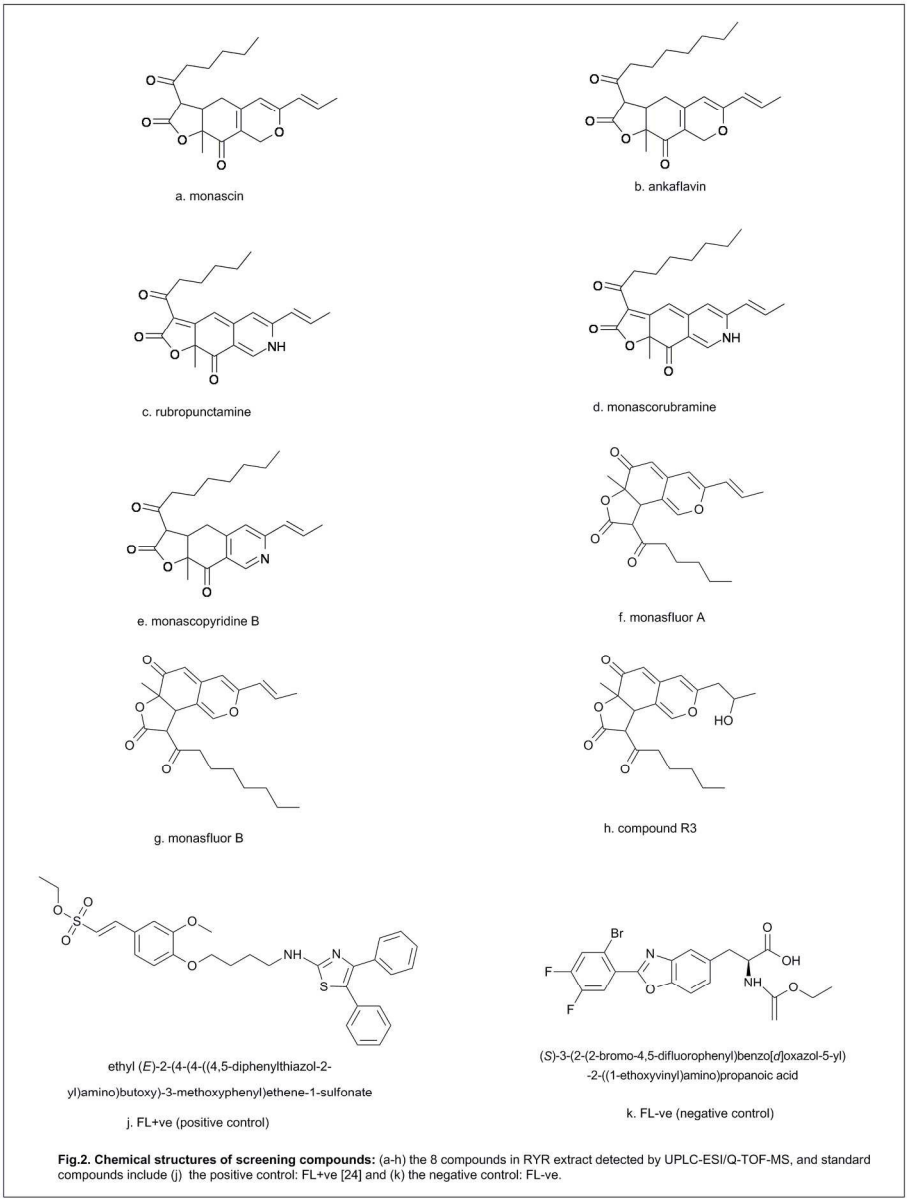

Fig.2. Chemical structures of screening compounds: (a-h) the 8 compounds in RYR extract detected by UPLC-ESI/Q-TOF-MS, and standard compounds include (j) the positive control: FL+ve [24] and (k) the negative control: FL-ve.

175x231mm (300 x 300 DPI)

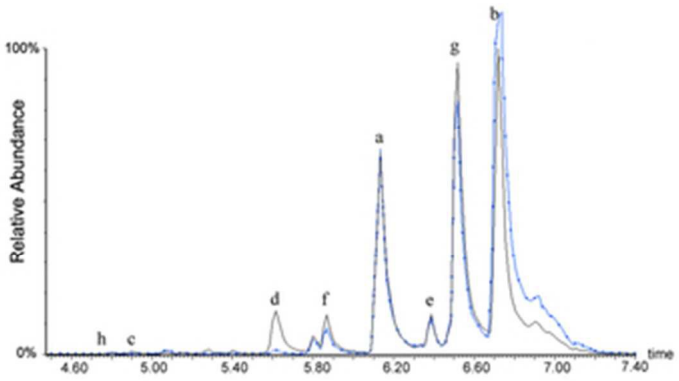

Fig. 3. LC traces of the 8 detectable compounds in the RYR extract mixed with (solid line) and without PTP1B (dotted line) after 3 rounds of ultrafiltration: a, monascin (Rt = 6.17 min); b, ankaflavin (Rt = 6.75 min); c, rubropunctamine (Rt = 4.91 min); d, monascorubramine (Rt = 5.63 min); e, monascopyridine B (Rt = 6.42 min); f, monasfluor A (Rt = 5.89 min); g, monasfluor B (Rt = 6.55 min); and h, compound R3 (Rt = 4.78 min).
28x15mm (300 x 300 DPI)

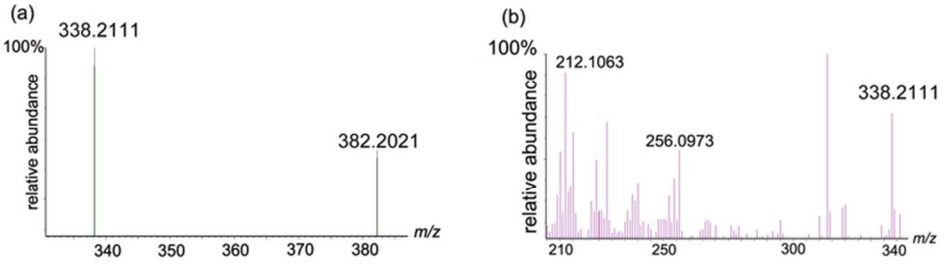

Fig. 4. (a-b) MSE spectra of monascorubramine in the positive ion mode;
68x21mm (300 x 300 DPI)

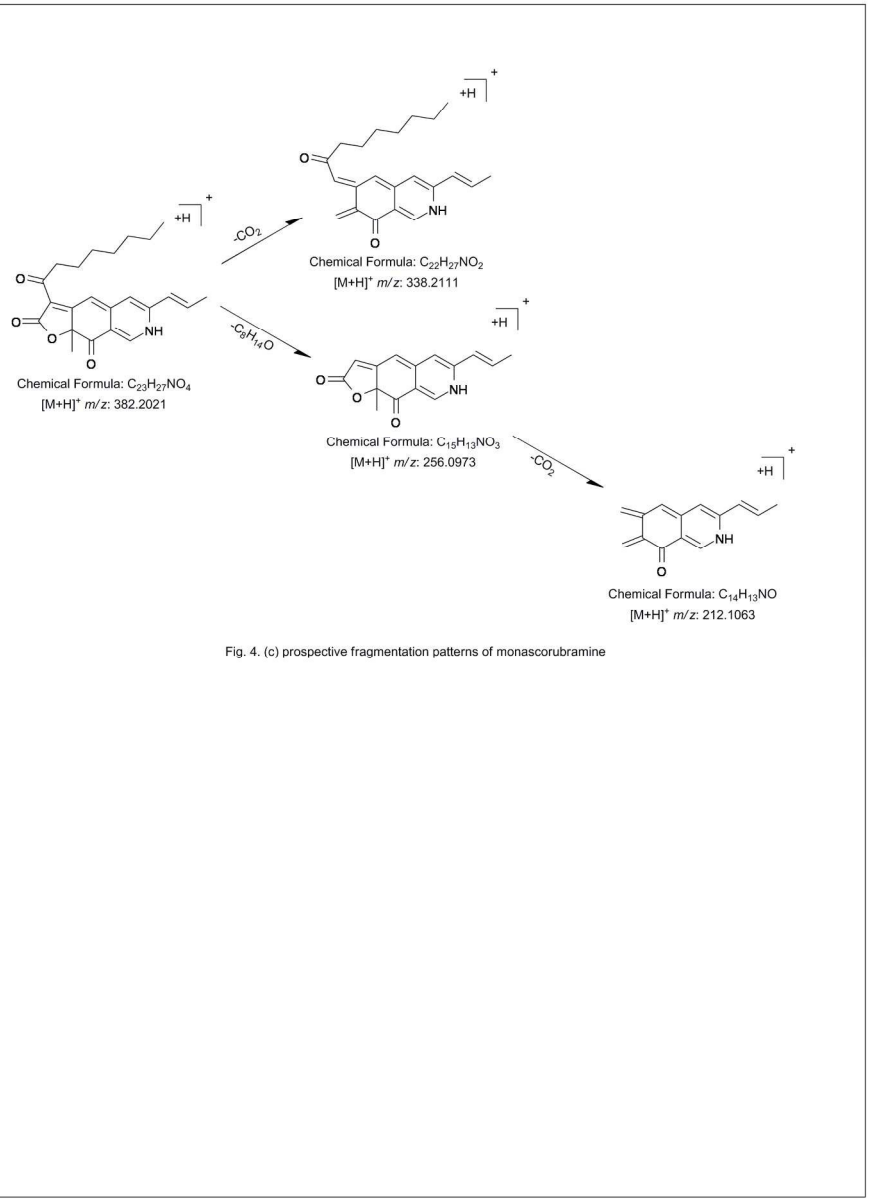

Fig. 4. (c) prospective fragmentation patterns of monascorubramine

175x231mm (300 x 300 DPI)

Graphic Table

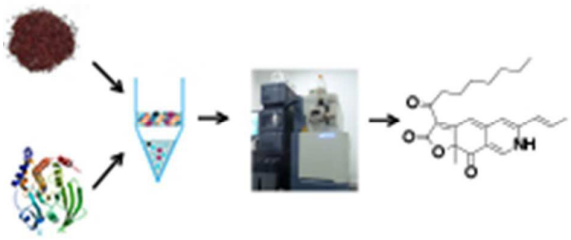

Highlight

Ultrafiltration-based affinity selection mass spectrometry was utilized to rapidly screen potential PTP1B inhibitors in Chinese red yeast rice.